Exciton diffusion in energetically disordered organic materials

Stavros Athanasopoulos,[1,*] Evguenia V. Emelianova,[1] Alison B. Walker,[2] and David Beljonne[1]
[1]*Laboratory for Chemistry of Novel Materials, University of Mons, Place du Parc 20, B-7000 Mons, Belgium*
[2]*Department of Physics, University of Bath, Bath BA2 7AY, United Kingdom*
(Received 11 June 2009; revised manuscript received 21 August 2009; published 19 November 2009)

We implement a simple, continuous, analytical model for exciton hopping in an energetically disordered molecular landscape. The model is parameterized against atomistic and lattice Monte Carlo simulations based on quantum-chemical calculations. It captures the essential physics of exciton diffusion in disordered media at different temperatures and yields a universal scaling law of the diffusion length with the dimensionless disorder parameter given by the ratio of the energetic disorder width to the thermal energy.

DOI: 10.1103/PhysRevB.80.195209 PACS number(s): 71.35.−y, 61.43.Bn, 71.20.Rv, 72.20.Ee

I. INTRODUCTION

Organic polymeric and molecular solids have emerged as promising materials in optoelectronic device applications.[1–3] The ability to control the way that charges and excitations move in organic materials is of paramount importance for the operation and efficiency of these devices. For example, in photovoltaic (PV) devices the dissociation of the initially formed excitation into charge carriers depends critically on the micro(meso)scopic structure. The average distance that an excitation can travel during its lifetime, the exciton diffusion length L_D, dictates whether the quasiparticle will reach the interface between the donor and the acceptor material where it might be energetically favorable to dissociate into the constituent charges.[4–6] Those charges have to find their way to the electrodes in order to contribute to the photocurrent. Depending on the morphology of the (blend) material, primary and secondary geminate recombination can greatly reduce the number of charges collected with respect to the number of the photons absorbed.[7] For high charge collection efficiencies, percolation pathways for the charges must exist through the device and recombination should be limited. The need to reconcile the competing processes of exciton dissociation and charge collection has led to the development of bulk heterojunction solar cells that incorporate an interpenetrating network of blended materials. In these structures, a happy medium is found giving optimal performance at an intermediate phase separation scale of the donor and the acceptor.[8] Compared to the corresponding multilayer architectures, the structures show a more complex morphology with limited control and reproducibility, which affects the resulting device performance. Hence L_D is one of the key parameters determining the internal quantum efficiency of organic PV cells.

Experimental assessment of exciton diffusion lengths in organic materials includes measurements of exciton-exciton annihilation,[9–11] microwave conductivity,[12,13] heterojunction photocurrent,[14–16] and photoluminescence quenching experiments,[17–23] with the latter being the most commonly used method. Those experiments have shown that L_D in conjugated polymers (CPs) is rather low, spanning a 5–10 nm range. It is at first surprising that all conjugated polymers feature similar L_D values, regardless of their chemical structure and solid-state packing. For instance, regioregular polyhexylthiophene (P3HT), despite being a semicrystalline material with high charge-carrier mobilities,[3] displays a value of L_D that is comparable to that of amorphous conjugated polymers.[10] On the other hand, much larger L_D values[12,16,23–25] have been reported in molecular materials and carbon nanotubes that are chemically more well-defined than CPs due to the distribution of physical and conjugation lengths in the latter. Therefore the underlying reason limiting exciton diffusion in conjugated polymers might be related to the static disorder in these materials. In CPs, disorder is large with respect to the electronic interactions that are responsible for the exciton delocalization and transport. On the contrary, in small molecules, due to the inverse length dependence of the excitonic coupling[26] the electronic interactions win over disorder, so that, transport-wise molecular materials are seemingly less vulnerable to disorder effects. Note that disorder can be either intrinsic (e.g., distribution of conformers) or extrinsic (e.g., induced by chemical defects) and encompasses both energetic and positional contributions. Although disorder is widely recognized to play a critical role in the transport properties of CPs, for energy diffusion this link has not been explored in great detail.

Various theoretical models that retain different levels of the geometric and electronic structures details have been employed to describe exciton transport in organic materials[27–35] and photosynthetic systems.[36–39] We have recently shown that the presence of traps limits exciton diffusion in conjugated polymers.[40] In this paper, we demonstrate that energetic disorder alone reduces L_D over more than one order of magnitude, from values typically encountered for molecules (>50 nm) to values actually measured in CP (<10 nm). The structure of the paper is as follows: first we develop analytical models for exciton hopping at high temperature T (equilibrium case) and at low T (nonequilibrium case). Next we apply these analytical models and compare the results to Monte Carlo (MC) simulations employing quantum-chemical calculations of the transfer rates in the specific case of polyindenofluorenes and rod morphology and a simplified version of these simulations where sites are voxels on a cubic lattice and Förster transfer rates are used. Remarkably, the three different approaches yield a similar picture of the influence of the degree of inhomogeneity on L_D, which follows a universal dependence on the T-renormalized disorder width.

II. EQUILIBRIUM HOPPING MODEL

The Förster energy-transfer rate, $\Gamma(E,E',r)$, between an occupied molecule/conjugated segment with energy E to a target molecule/conjugated segment of energy E' separated by distance r is given by:

$$\Gamma(E,E',r) = \frac{1}{\tau}\left[\frac{r_F}{r}\right]^6 \times \begin{cases} \exp\left(-\dfrac{E'-E}{kT}\right), & E' > E \\ 1, & E' < E \end{cases}, \tag{1}$$

where r_F is the Förster radius, τ is the lifetime of the excitation, T is the temperature, and k the Boltzmann constant. The Boltzmann weighting factor for a transfer upwards in energy ensures the detailed balance requirements.[28] The hopping rate can be written as a function of the hopping parameter u (as it was done in Ref. 41 for the Miller-Abrahams hopping rate of charge carriers): $\Gamma = \frac{1}{\tau}\exp[-u]$, where $u(E,E',r) = 6\ln(\frac{r}{r_F}) + \frac{\eta(E'-E)}{kT}$, with η the unit step (Heaviside) function. If hopping sites are found at random positions, the average number of target sites for an occupied molecule of energy E with hopping parameters $\leq u$ can be calculated by integration over all target site energies and distances for an exciton density of states $\rho(E) = N_t g(E)$, where N_t the total number of exciton states in unit volume, proportional to the spatial chromophore density:

$$\begin{aligned} n(E,u) &= 4\pi \int_0^{r_F \exp(u/6)} r^2 dr \int_{-\infty}^{E+kT(u-6\ln(r/r_F))} N_t g(E')dE' \\ &= 4\pi \int_{-\infty}^{E} N_t g(E')dE' \int_0^{r_F \exp(u/6)} r^2 dr \\ &\quad + 4\pi \int_E^{\infty} N_t g(E')dE' \int_0^{r_F \exp[1/6(u-E'/kT+E/kT)]} r^2 dr \\ &= \frac{4\pi}{3} r_F^3 N_t \exp(u/2)\left[\int_{-\infty}^{E} g(E')dE' \right. \\ &\quad \left. + \exp\left(\frac{E}{2kT}\right)\int_E^{\infty} g(E')\exp\left(-\frac{E'}{2kT}\right)dE'\right]. \end{aligned} \tag{2}$$

On the right-hand side of Eq. (2), the first and second terms give the number of target sites that have, respectively, lower and higher excitation energy than the starting site. The mean-square exciton hopping distance, $\langle r^2(E)\rangle$, can be evaluated as:

$$\begin{aligned} \langle r^2(E)\rangle &= \frac{4\pi \int_0^{r_F \exp(u/6)} r^2 r^2 dr \int_{-\infty}^{E+kT(u-6\ln(r/r_F))} g(E')dE'}{4\pi \int_0^{r_F \exp(u/6)} r^2 dr \int_{-\infty}^{E+kT(u-6\ln(r/r_F))} g(E')dE'} \\ &\cong r_F^2 \exp(\langle u(E)\rangle/3). \end{aligned} \tag{3}$$

An average hopping parameter, $\langle u(E)\rangle$, can be evaluated from the assumption that there is at least one target site in the neighborhood.[41] In the present model we assume an exciton density that is low compared to the density of exciton hopping sites. The equilibrium diffusion coefficient is obtained by multiplying $\langle r^2(E)\rangle$ with the hopping rate Γ averaged over E under thermal equilibrium conditions:[42]

$$\begin{aligned} D &= \frac{1}{\tau}\frac{\int_{-\infty}^{+\infty} g(E)\exp(-E/kT)\exp[-\langle u(E)\rangle]\langle r^2(E)\rangle dE}{\left[\int_{-\infty}^{+\infty} g(E)\exp(-E/kT)dE\right]} \\ &\cong \frac{r_F^6}{\tau}\left(\frac{4\pi N_t}{3}\right)^{4/3} \frac{\int_{-\infty}^{+\infty} g(E)\exp\left(-\dfrac{E}{kT}\right)dE}{\left[\int_{-\infty}^{+\infty} g(E)\exp(-E/kT)dE\right]} \\ &\quad \times \left[\int_{-\infty}^{E} g(E')dE' + \exp\left(\frac{E}{2kT}\right)\int_E^{+\infty} g(E') \right. \\ &\quad \left. \times \exp\left(-\frac{E'}{2kT}\right)dE'\right]^{4/3}. \end{aligned} \tag{4}$$

Using Eq. (4) one can easily calculate the exciton diffusion length as follows

$$L_D = \sqrt{D\tau} = r_F\left[\frac{\int_{-\infty}^{\infty} g(E)\exp(-E/kT)\exp\left(-\dfrac{2}{3}\langle u(E)\rangle\right)dE}{\int_{-\infty}^{\infty} g(E)\exp(-E/kT)}\right]^{1/2}. \tag{5}$$

Eq. (5) allows L_D to be determined for any $g(E)$. In what follows we will assume there are N_t sites per volume that have a Gaussian distribution in energy with a variance σ^2: $g(E) = \frac{1}{\sigma\sqrt{2\pi}}\exp(-\frac{E^2}{2\sigma^2})$. We stress that disorder is here assumed to be static, i.e., the time scale for the fluctuation in site energies is long compared to the hopping times.

III. ENERGY-DEPENDENT FÖRSTER RADIUS

In this section we generalize the model developed above to the case where the Förster radius r_F, defined in Eq. (1), depends on the energy E of the starting site. The average number of target sites is now:

$$\begin{aligned} n(E,u) &= 4\pi \int_{-\infty}^{E} \rho(E')dE' \int_0^{r_F(E)\exp[u/6]} r^2 dr \\ &\quad + 4\pi \int_E^{+\infty} \rho(E')dE' \int_0^{r_F(E')\exp[1/6(u+E/kT-E'/kT)]} r^2 dr \\ &= \frac{4\pi[r_F(E)]^3}{3}\exp\left[\frac{u}{2}\right]\left[\int_{-\infty}^{E} \rho(E')dE' \right. \\ &\quad \left. + \exp\left[\frac{E}{2kT}\right]\int_E^{\infty} \rho(E')\exp\left[-\frac{E'}{kT}\right]dE'\right], \end{aligned} \tag{6}$$

where $r_F(E)$ is now a function of the exciton starting energy. Hence, from Eqs. (3) and (4) the diffusion coefficient can be written as

$$D = \frac{1}{\tau}\left(\frac{4\pi N_t}{3}\right)^{4/3}\frac{3}{5}\frac{1}{\left[\int_{-\infty}^{+\infty} g(E)\exp(-E/kT)dE\right]}\int_{-\infty}^{\infty} dE \times \left[g(E)\exp\left(-\frac{E}{kT}\right)\left\{\int_{-\infty}^{E} g(E')[r_F(E')]^3 dE' + \exp\left(\frac{E}{2kT}\right)\int_{E}^{+\infty} g(E')[r_F(E')]^3\exp\left(-\frac{E'}{2kT}\right)dE'\right\}^{1/3} \times \left\{\int_{-\infty}^{E} g(E')[r_F(E')]^5 dE' + \exp\left(\frac{5E}{6kT}\right)\int_{E}^{+\infty} g(E') \times [r_F(E')]^5\exp\left(-\frac{5E'}{6kT}\right)\right\}\right]. \quad (7)$$

Both Eqs. (4) and (7) lead to the expected dependence of the diffusion coefficient: $D \sim \frac{r_F^6}{\tau} N_t^{4/3}$.[43] Henceforth L_D scales as the third power of the Förster radius r_F and as the 2/3 power of the chromophore density N_t.

IV. NONEQUILIBRIUM HOPPING MODEL

At low temperatures the hopping transport of vibronically relaxed excitons occurs under nonequilibrium conditions as the relaxation time is much larger than the lifetime of the excitation and excitons predominantly make downward hops in the manifold of the exciton energy states since thermally activated upward jumps are less probable. The kinetics of the spectral diffusion of a vibronically relaxed exciton has been described by Arkhipov *et al.*[44] In this reference, the nonequilibrium energy distribution function $f(E,r,t)$ of the excitons, which have energy E at time t and a nearest neighbor with lower energy at distance r was derived:

$$f(E,r,t) = A(t)r^2\rho(E)N(E)\exp\left[-\frac{4\pi r^3}{3}N(E) - \frac{t}{\tau}\left(\frac{r_F(E)}{r}\right)^6\right] \quad (8)$$

with $A(t)$ a normalization constant:

$$A(t) = \exp\left(-\frac{t}{\tau}\right)\left\{\int_0^{+\infty} r^2 dr \int_{-\infty}^{\infty} \rho(E)N(E) \times \exp\left[-\frac{4\pi r^3}{3}N(E) - \frac{t}{\tau}\left(\frac{r_F(E)}{r}\right)^6\right]dE\right\}^{-1} \quad (9)$$

$N(E)$ is the density of excitonic states with energy smaller than E

$$N(E) = \int_{-\infty}^{E} \rho(E')dE'. \quad (10)$$

Using $f(E,r,t)$, one can calculate the exciton hopping rate $\Gamma(t)$ and the number of hops $n(t)$ an exciton has performed from time t until it decays [see Eqs. 10 and 11 in Ref. 44], as well as the total number of hops, $n(t=0)$. L_D can be estimated as

$$L_D = \sqrt{\langle r^2\rangle n(t=0)}, \quad (11)$$

where $\langle r^2\rangle$ can be calculated using the distribution function $f(E,r,t)$ as follows:

$$\langle r^2\rangle = \frac{1}{\tau}\int_0^{\tau} dt \int_0^{\infty} r^2 dr \int_{-\infty}^{\infty} f(E,r,t)dE. \quad (12)$$

As a first approximation, one might assume a constant Förster radius, which is averaged through the energy distribution of the exciton target hopping sites. However, L_D could be significantly overestimated at low temperatures if the energy variation of the Förster radius is neglected. The fastest exciton hops are performed while the starting energy is near the center of the distribution where the probability of finding a neighbor is very high so traverse the smallest distances. After a few downward jumps the probability of finding a neighbor to which a jump is probable has decreased noticeably so the hopping rate becomes much smaller than its averaged value. For a better estimate of L_D, we allow r_F to vary with E. Since the hopping rate strongly decreases with increasing distance, most excitations will jump to the nearest available neighbors. Employing the expression for $f(E,r,t)$ in Eq. (8) one can calculate the total jump rate Γ_{tot} as a function of time using:

$$\Gamma_{\text{tot}}(t) = \frac{1}{\tau}\int_0^{\infty} dr \int_{-\infty}^{\infty} \left(\frac{r_F(E)}{r}\right)^6 f(E,r,t)dE. \quad (13)$$

Integrating Eq. (13) over time from $t=0$ to infinity yields the average number of jumps $n(t=0)$ the exciton has performed during its lifetime. The exciton diffusion length can then be deduced from Eq. (11).

V. COMBINED QUANTUM-CHEMICAL CALCULATIONS AND MONTE CARLO SIMULATIONS

To compare the analytical results with material specific calculations, we perform a kinetic MC scheme of exciton diffusion with quantum-chemical calculations of the transfer rates. A detailed description of the approach and its application can be found in reference.[40] Briefly, we consider a crystalline assembly of polyindenofluorene polymer chains parallel to each other that pack with their chain midpoints forming a hexagonal lattice. Each chain consists of a distribution of chromophore units, from trimers up to octamers, which is derived by fitting the experimental absorption spectra. Here we will assume that the energy of each site is randomly chosen from a Gaussian distribution with standard deviation σ. The transfer rates between chromophore units are calculated using an improved Förster model, which takes into account the spatial extent of the excited state wave function, and involve the product of the excitonic coupling and spectral overlap between a donor site r_i and an acceptor site r_j:[45]

$$\Gamma_{ij} = 1.18|V_{ij}|^2 J_{ij}, \quad (14)$$

where V_{ij} is the electronic coupling in cm^{-1} and J_{ij} the overlap between the donor fluorescence $F_i(\omega)$ and acceptor absorption spectrum $A_j(\omega)$ normalized in cm^{-1} given by

$$J_{ij} = \int_0^\infty F_i(\omega) A_j(\omega) d\omega. \tag{15}$$

The simulated absorption and emission spectra were obtained at the INDO/SCI level within the Frank-Condon approximation and a displaced harmonic oscillator model. Two effective vibrational modes have been considered for the coupling to the excited state, a high frequency mode at 1300 cm^{-1} and a low-frequency vibrational mode at 80 cm^{-1}. The spectra have been broadened by a Lorentzian lineshape with a linewidth of 0.04 eV.

We have employed the distributed monopole model[45] to calculate the excitonic coupling V_{ij} between molecular units i and j, which is expressed as a Coulombic term

$$V_{ij} = \frac{1}{4\pi\varepsilon_0} \sum_{a \neq d} \frac{\rho_i(\vec{r}_d)\rho_j(\vec{r}_a)}{|\vec{r}_d - \vec{r}_a|}, \tag{16}$$

where ε_0 the vacuum permittivity, r_d and r_a denote the donor and acceptor atomic positions respectively over which the sums runs and ρ the atomic transition densities computed at the INDO/SCI[46] level. Assuming that there are no nonradiative paths to the ground state, the excited-state lifetime τ has been estimated as the inverse of the Einstein coefficient for spontaneous emission with the frequency of the transition and the dipole moment obtained from the INDO/SCI calculations.

The transfer rates are employed in a kinetic MC scheme where the dynamics of the exciton transport is modeled as a stochastic process. Excitons are either created at random sites within the assembly or at sites of a given energy in the case of energy selective excitation. These excitations could either hop to a nearest-neighbor site or decay. To account for the hopping events that contribute to the transport of the excitation, a time for the excitation at site i to transfer to any of the available target sites j is calculated from an exponential distribution

$$\tau_{ij} = -\frac{1}{\Gamma_{ij}} \ln(X), \tag{17}$$

with X a random number uniformly distributed between 0 and 1. In a similar fashion a recombination time is calculated as $\tau_r = -\tau \ln(X)$, where τ is the lifetime of the excitation. All the possible events are placed into a list and the event with the smallest waiting time is chosen at each MC step. If the chosen event is a hop, the excitation moves to the selected site and a new set of dwell times is calculated. If the chosen event is decay the exciton is removed from the system and a new exciton trial starts. We perform 10 000 trials for each disorder realization and temperature. Since we monitor the position of all excitations from the starting to the final position, an average value for L_D can be extracted from the simulations. We should emphasize that this is a direct way of calculating L_D without the need to estimate a diffusion coefficient from, e.g., a linear fit to the mean square displacement at large simulation times. For an energetically disordered system where there is a crossover time to the linear diffusive regime[47,48] the latter approach potentially overestimates L_D.[49] An equally misleading situation in evaluating diffusion lengths via a constant diffusion coefficient occurs in low-temperature simulations where the excitons never enter the normal diffusive regime and D decreases with time.

In addition to the MC simulations with transfer rates from quantum-chemical calculations we also perform MC simulations where sites are voxels on a cubic lattice with a lattice constant of 1 nm, site energies are distributed according to a Gaussian with width σ; Förster transfer rates between the sites are given by Eq. (1); the Förster radius is extracted from the quantum-chemical calculations of the transfer rates between indenofluorene oligomers and the radiative lifetime is 500 ps (the radiative lifetime averaged over the population for all oligomers). This approach is less demanding and allows us to examine the impact of energetic disorder on exciton diffusion in a positionally ordered system. Simulation cells of up to 125 000 sites with periodic boundary conditions are used.

VI. RESULTS AND DISCUSSION

Our main results are summarized in Fig. 1 where at the top panel we depict L_D for different values of σ for the analytical model and the MC simulations. The analytical and cubic lattice MC results are based on a Förster radius of 3.1 nm extracted from the quantum-chemical calculations while the parametric dependence of L_D on the Förster radius is shown in the inset. The analytical model provides similar values for L_D once the energy dependence of the Förster radius is taken into account. We find that there is a good agreement between the analytical and numerical results. In particular, increasing σ results in a reduction of L_D. Since at room-temperature excitons occupy states at the thermal level $E_{th} = -\sigma^2/\kappa T$, this level shifts for increasing disorder strength σ toward the bottom of the density of states where it is difficult to find nearest neighbors to hop to. Additionally, we show that it is important to take into account exciton hops to neighbors located at distances at least equal to the Förster radius as a failure to do so results in an underestimate of L_D. This is because by restricting exciton hopping to nearest neighbor sites which may not be energetically favorable, we do not allow for long distance hops that have smaller energy barriers. We find that for values of σ between 0.08 and 0.1 eV the exciton diffusion length is reduced to 5–10 nm, values that are typically found for conjugated polymers, see above. Such values of the energetic disorder are of the order of magnitude measured in conjugated polymers.[28,50] We observe that as disorder becomes stronger, the increase of L_D with increasing r_F becomes less pronounced. For high values of disorder L_D would hardly increase with increasing r_F [see top panel in Fig. 1 (inset)].

The bottom panel of Fig. 1 confirms that the quantum-chemical-based MC simulations of L_D agree with the nonequilibrium hopping model at low temperatures and at these temperatures L_D is sensitive to the excitation energy as seen experimentally.[51,52] At low T, exciton transport takes place under nonequilibrium conditions where excitons preferably move downwards in energy, performing a small number of hops (as shown in the inset), and with a decrease in the transfer rates as a function of time, as the next jump occurs

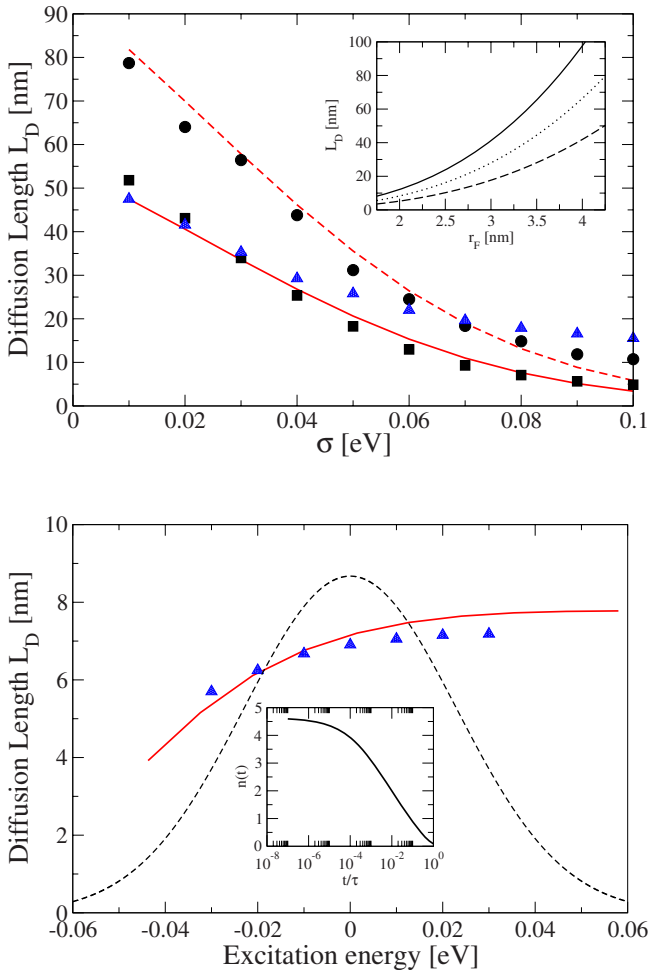

FIG. 1. (Color online) Top panel: L_D as a function of the standard deviation σ of the energy distribution at $T=294$ K. Lines show the equilibrium hopping model including first (straight line) and second (dashed line) nearest neighbors. Symbols are from MC simulations: a cubic lattice morphology with Förster transfer rates and only nearest-neighbor hops (squares) and up to third nearest-neighbor hops (circles); a chain morphology with transfer rates calculated at the quantum-chemical level (triangles up). The inset shows the parametric dependence of L_D on the Förster radius from the equilibrium model (see Eq. (5)) for $\sigma=0.02$ eV (solid line), 0.04 eV (dotted line), and 0.06 eV (dashed line). Bottom panel: L_D at $T=7$ K for different excitation energies in a Gaussian density of states (shown not normalized as a dashed line) with $\sigma=0.023$ eV for the nonequilibrium hopping model (solid line) and the MC simulations with quantum-chemical rates (triangles up). The number of exciton hops n vs time t scaled by the decay time τ for the nonequilibrium model is shown in the inset.

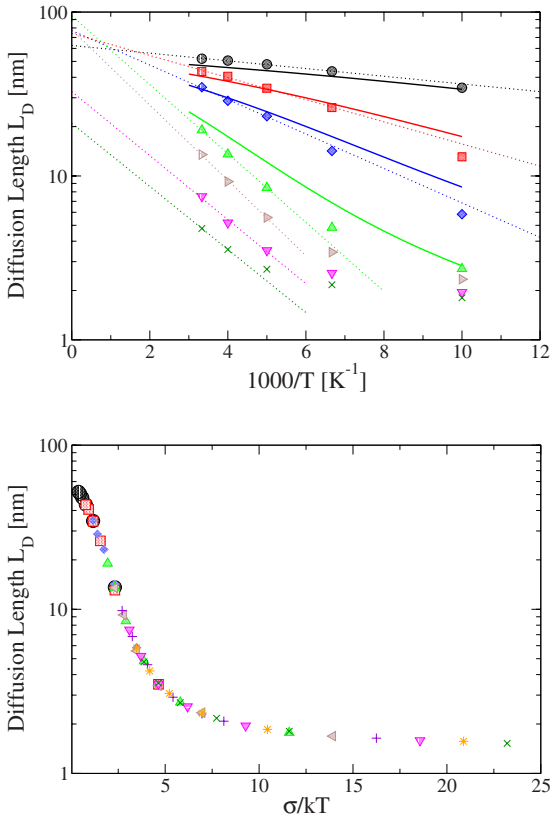

FIG. 2. (Color online) Top panel: Arrhenius plot of L_D for the equilibrium hopping model (straight line) and the cubic lattice MC simulations with Förster transfer rates for σ in eV of (circles), 0.02 (squares), 0.03 (diamonds), 0.05 (up triangles), 0.06 (sideways triangles), 0.08 (down triangles), and 0.1 (crosses). Dashed lines represent the Arrhenius fit to the MC results at high T. Bottom panel: L_D variation with the dimensionless disorder parameter σ/kT. Symbols are as for the top panel and σ in eV of 0.07 (plus signs), and 0.09 eV (asterisks).

to a more distant site. Thus, excitons created deep in the low-energy tail of $\rho(E)$ will travel shorter distances than excitons generated in the middle of $\rho(E)$. Energy selective measurements of L_D at low T could provide a method of distinguishing whether the diffusion is limited by the presence of traps[40,53] or by the presence of energetic disorder.

L_D is expected to decrease with decreasing temperature as thermally activated hops become less frequent. In Fig. 2 we demonstrate that L_D depends sensitively on σ and T, showing Arrhenius behavior for low σ and high T, with an activation energy that increases with σ. The equilibrium hopping model, within the range of validity (low disorder, high T), agrees with the MC simulations. However, L_D becomes less sensitive to T than predicted by the equilibrium hopping model for high disorder levels. A different temperature dependence is predicted at low T, where transport takes place under nonequilibrium conditions and the diffusion length saturates. It is interesting to note that our findings agree with recent temperature dependent measurement of L_D in MDMO-PPV (poly[2-methyl-5-(3',7'-dimethyloctyloxy)-p phenylenevinylene]) samples by Blom *et al.*[17]

For small values of σ the decrease in L_D with temperature is moderate whereas L_D decays rapidly for large values of σ. It is therefore a combination of σ and T that controls L_D. This result is confirmed by the bottom panel of Fig. 2, which shows that L_D scales with σ/kT, as was found for charge-carrier mobility in organic semiconductors.[54,55] The scaling of L_D with σ/kT also follows directly from the analytical model as can be seen in Eq. (5) for a Gaussian excitonic density of states $g(E)$. This scaling could provide means of either predicting L_D for any combination of T and σ once L_D is known for a given temperature or a way of measuring the disorder present in the material by measuring L_D.

VII. CONCLUSIONS

We have studied the dynamics of exciton diffusion in disordered organic molecular solids, comparing an analytical model with a Monte Carlo model employing transfer rates from quantum-chemical calculations or Förster theory. We find that given its simplicity and limitations, the analytical hopping model can provide a good description of exciton transport with respect to the more accurate quantum-chemical/Monte Carlo approach when the assumption of equilibrium at high temperatures is avoided at low temperatures. Moreover, we demonstrate that energetic disorder plays an important role by slowing down diffusion and its presence is sufficient to limit the values of exciton diffusion length even in the absence of positional disorder. This result could explain the very small variability of experimentally determined exciton diffusion lengths in chemically different polymers and also the much larger diffusion lengths measured in small molecules. It should be emphasized here that the excitonic coupling, which is a subtle function of the relative molecular arrangements and conjugation length, is also a critical parameter controlling the exciton dynamics. However, high values of disorder tend to wash out any improvements that would be expected based on increasing the Förster radius. Additionally we demonstrate that in a system with energetic disorder the exciton diffusion length depends on the excitation wavelength. Finally we predict a scaling of the diffusion length with the dimensionless disorder parameter.

ACKNOWLEDGMENTS

The work has been partly supported by the European Commission STREP project No. MODECOM (NMP-CT-2006-016434), by the Belgian Science Policy (program IAP, P6/27), and by the Belgian Research Science Foundation (FNRS and FRFC through the Interuniversity Scientific Calculation Facility, ISCF). D.B. is Research Director at FNRS. E.E. would like to acknowledge discussions with V. I. Arkhipov.

*stavrosa@averell.umh.ac.be

[1] G. Li, V. Shrotriya, J. S. Huang, Y. Yao, T. Moriarty, K. Emery, and Y. Yang, Nature Mater. **4**, 864 (2005).
[2] P. Peumans, A. Yakimov, and S. R. Forrest, J. Appl. Phys. **93**, 3693 (2003).
[3] H. Sirringhaus *et al.*, Nature (London) **401**, 685 (1999).
[4] J. S. Kim *et al.*, J. Am. Chem. Soc. **130**, 13120 (2008).
[5] Y. S. Huang, S. Westenhoff, I. Avilov, P. Sreearunothai, J. M. Hodgkiss, C. Deleener, R. H. Friend, and D. Beljonne, Nature Mater. **7**, 483 (2008).
[6] M. C. Scharber, D. Wuhlbacher, M. Koppe, P. Denk, C. Waldauf, A. J. Heeger, and C. L. Brabec, Adv. Mater. **18**, 789 (2006).
[7] P. W. M. Blom, V. D. Mihailetchi, L. J. A. Koster, and D. E. Markov, Adv. Mater. **19**, 1551 (2007).
[8] P. K. Watkins, A. B. Walker, and G. L. B. Verschoor, Nano Lett. **5**, 1814 (2005).
[9] A. J. Lewis, A. Ruseckas, O. P. M. Gaudin, G. R. Webster, P. L. Burn, and I. D. W. Samuel, Org. Electron. **7**, 452 (2006).
[10] P. E. Shaw, A. Ruseckas, and I. D. W. Samuel, Adv. Mater. **20**, 3516 (2008).
[11] M. A. Stevens, C. Silva, D. M. Russell, and R. H. Friend, Phys. Rev. B **63**, 165213 (2001).
[12] A. Huijser, T. J. Savenije, S. C. J. Meskers, M. J. W. Vermeulen, and L. D. A. Siebbeles, J. Am. Chem. Soc. **130**, 12496 (2008).
[13] J. E. Kroeze, T. J. Savenije, M. J. W. Vermeulen, and J. M. Warman, J. Phys. Chem. B **107**, 7696 (2003).
[14] J. J. M. Halls, K. Pichler, R. H. Friend, S. C. Moratti, and A. B. Holmes, Appl. Phys. Lett. **68**, 3120 (1996).
[15] L. A. A. Pettersson, L. S. Roman, and O. Inganas, J. Appl. Phys. **86**, 487 (1999).
[16] S. Yoo, B. Domercq, and B. Kippelen, Appl. Phys. Lett. **85**, 5427 (2004).
[17] O. V. Mikhnenko, F. Cordella, A. B. Sieval, J. C. Hummelen, P. W. M. Blom, and M. A. Loi, J. Phys. Chem. B **112**, 11601 (2008).
[18] M. Stoessel *et al.*, J. Appl. Phys. **87**, 4467 (2000).
[19] D. E. Markov, E. Amsterdam, P. W. M. Blom, A. B. Sieval, and J. C. Hummelen, J. Phys. Chem. A **109**, 5266 (2005).
[20] S. R. Scully and M. D. McGehee, J. Appl. Phys. **100**, 034907 (2006).
[21] D. E. Markov, C. Tanase, P. W. M. Blom, and J. Wildeman, Phys. Rev. B **72**, 045217 (2005).
[22] A. Haugeneder, M. Neges, C. Kallinger, W. Spirkl, U. Lemmer, J. Feldmann, U. Scherf, E. Harth, A. Gugel, and K. Mullen, Phys. Rev. B **59**, 15346 (1999).
[23] A. Mani, J. Schoonman, and A. Goossens, J. Phys. Chem. B **109**, 4829 (2005).
[24] M. Stella, C. Voz, J. Puigdollers, F. Rojas, A. Fonrodona, J. Escarre, J. M. Asensi, J. Bertomeu, and J. Andreu, J. Non-Cryst. Solids. **352**, 1663 (2006).
[25] C. X. Sheng, Z. V. Vardeny, A. B. Dalton, and R. H. Baughman, Phys. Rev. B **71**, 125427 (2005).
[26] J. Gierschner, Y. S. Huang, B. Van Averbeke, J. Cornil, R. H. Friend, and D. Beljonne, J. Chem. Phys. **130**, 044105 (2009).
[27] S. Westenhoff, C. Daniel, R. H. Friend, C. Silva, V. Sundstrom, and A. Yartsev, J. Chem. Phys. **122**, 094903 (2005).
[28] S. C. J. Meskers, J. Hubner, M. Oestreich, and H. Bassler, J. Phys. Chem. B **105**, 9139 (2001).
[29] C. Didraga, V. A. Malyshev, and J. Knoester, J. Phys. Chem. B **110**, 18818 (2006).
[30] V. M. Burlakov, K. Kawata, H. E. Assender, G. A. D. Briggs, A. Ruseckas, and I. D. W. Samuel, Phys. Rev. B **72**, 075206 (2005).
[31] G. D. Scholes and G. Rumbles, Nature Mater. **5**, 683 (2006).
[32] W. Barford, J. Chem. Phys. **126**, 134905 (2007).
[33] W. Barford and C. D. P. Duffy, Phys. Rev. B **74**, 075207 (2006).
[34] G. Schnönherr, R. Eiermann, H. Bässler, and M. Silver, Chem. Phys. **52**, 287 (1980).
[35] C. Madigan and V. Bulovic, Phys. Rev. Lett. **96**, 046404 (2006).
[36] J. M. Jean, C. K. Chan, G. R. Fleming, and T. G. Owens, Biophys. J. **56**, 1203 (1989).
[37] G. Trinkunas and A. R. Holzwarth, Biophys. J. **66**, 415 (1994).

[38] Y. W. Jia, J. M. Jean, M. M. Werst, C. K. Chan, and G. R. Fleming, Biophys. J. **63**, 259 (1992).
[39] T. Pullerits and A. Freiberg, Biophys. J. **63**, 879 (1992).
[40] S. Athanasopoulos, E. Hennebicq, D. Beljonne, and A. B. Walker, J. Phys. Chem. C **112**, 11532 (2008).
[41] V. I. Arkhipov, E. V. Emelianova, and G. J. Adriaenssens, Phys. Rev. B **64**, 125125 (2001).
[42] V. I. Arkhipov, E. V. Emelianova, and H. Bässler, Philos. Mag. B **81**, 985 (2001).
[43] T. S. Ahn, N. Wright, and C. J. Bardeen, Chem. Phys. Lett. **446**, 43 (2007).
[44] V. I. Arkhipov, E. V. Emelianova, and H. Bassler, Chem. Phys. Lett. **383**, 166 (2004).
[45] E. Hennebicq *et al.*, J. Am. Chem. Soc. **127**, 4744 (2005).
[46] J. Ridley and M. Zerner, Theor. Chim. Acta **32**, 111 (1973).
[47] I. Avramov, A. Milchev, and P. Argyrakis, Phys. Rev. E **47**, 2303 (1993).
[48] A. Horner, A. Milchev, and P. Argyrakis, Phys. Rev. E **52**, 3570 (1995).
[49] K. M. Gaab and C. J. Bardeen, J. Phys. Chem. A **108**, 10801 (2004).
[50] T. Pullerits, O. Mirzov, and I. G. Scheblykin, J. Phys. Chem. B **109**, 19099 (2005).
[51] K. M. Gaab and C. J. Bardeen, J. Phys. Chem. B **108**, 4619 (2004).
[52] A. D. Stein, K. A. Peterson, and M. D. Fayer, J. Chem. Phys. **92**, 5622 (1990).
[53] M. Schlosser and S. Lochbrunner, J. Phys. Chem. B **110**, 6001 (2006).
[54] H. Bässler, Phys. Status Solidi B **175**, 15 (1993).
[55] H. Bassler, Int. J. Mod. Phys. B **8**, 847 (1994).